

Trading styles and long-run variance of asset prices

Lawrence Middleton*, James Dodd*, Simone Rijavec*†

September 20, 2021

Abstract

Trading styles can be classified into either trend-following or mean-reverting. If the net trading style is trend-following the traded asset is more likely to move in the same direction it moved previously (the opposite is true if the net style is mean-reverting). The result of this is to introduce positive (or negative) correlations into the time series. We here explore the effect of these correlations on the long-run variance of the series through probabilistic models designed to explicitly capture the direction of trading. Our theoretical insights suggests that relative to random walk models of asset prices the long-run variance is increased under trend-following strategies and can actually be *reduced* under mean-reversal conditions. We apply these models to some of the largest US stocks by market capitalisation as well as high-frequency EUR/USD data and show that in both these settings, the ability to predict the asset price is generally *increased* relative to a random walk.

1 Background and related literature

The variance of a financial asset is a proxy for how predictable the asset is after some given period. The following aims to quantify the change in variance of an instrument under the simplifying assumption that the price dynamics are governed by either prevailing trend-following strategies or prevailing mean-reverting strategies. On the one hand, if the overall view of the market is momentum based then an increase in the price on any trading day is likely to increase the share price on the following day [Chan et al., 1996, Jegadeesh and Titman, 2001]. Conversely, if the overall view of the market is mean reverting then an increase is likely to be followed by a successive decrease the following day. Importantly, the former mimics the typical scenario arising in passive investment, where for example additional positive investment follows initially favourable conditions thereby driving up the price of the asset. In the following, we investigate how each of these styles impacts the overall variance of an instrument.

*Research sponsored by The Witness Corporation (www.thewitnesscorporation.com)

†University of Oxford, Department of Physics

We explore this probabilistically through examining a *correlated random walk* [Renshaw and Henderson, 1981] - a model such that the returns take values either -1 or +1 and where a day's closing returns is equal to the previous day's with probability p . Such a model touches on random walk theory for asset pricing. There exists a long history of using random walks in finance and econophysics [Fama, 1995, Sewell, 2011, Scalas, 2006b], a full review is beyond the scope of this article. Of note also, random walk models appear in the evaluation of the Efficient Market Hypothesis [Malkiel, 2003, Malkiel and Fama, 1970] where the predictability of a process is central to establishing whether markets are efficient or not.

In addition to the simplistic model, we consider two models applicable to financial assets over different return horizons. We consider firstly daily US stock data where after developing and validating an appropriate model we estimate the probability of each stock moving in the same direction on subsequent days. Exploiting this, we are able to quantify the change in variance relative to a random walk for each of the assets and thereby show that the variance is *deflated* in most of these stocks. We also test the prediction accuracy of a similar model on a week's worth of high-frequency EUR/USD where we are able to conclude again that the net trading style is mean-reverting and to a more exaggerated extent than the daily stock data.

2 Simulation study

We consider two discretet-time stochastic process models for asset prices (X_t) and (Y_t) for $t = 0, 1, \dots$. The first, (RW) is a random walk where $\mathbb{P}[X_{t+1} = X_t + 1] = \mathbb{P}[X_{t+1} = X_t - 1] = \frac{1}{2}$. The second, random walk (CRW) is a random walk with persistence in the direction it travels, i.e., Y_t for $t = 0, 1, \dots$

1. If $Y_t = Y_{t-1} + 1$ (last move was up) then $Y_{t+1} = Y_t + 1$ (next move will be up) with probability p
2. If $Y_t = Y_{t-1} - 1$ (last move was down) then $Y_{t+1} = Y_{t-1} - 1$ (next move will be down) with probability p

We plot these two situations in Figure 1, simulating 1000 realisations of each of the two models over 1,000 units of time, setting $p = \frac{1}{4}$ and $p = \frac{3}{4}$ for CRW and where the initial directions were distributed randomly up and down with probability 1/2. We see that there appears to be a relative increase in the variance of the assets for the random walk with persistence compared to that without when $p = \frac{3}{4}$ and a relative decrease when $p = \frac{1}{4}$. As a result, we look at the standard deviation of each of the two models through time in Figure 2a where we see the standard deviation is close to double that of the random walk model when $p = \frac{3}{4}$. Indeed, in Figure 2b the variance (square of std. deviation.) is approximately linear in both cases.

Next, we examine the relative increase in variance between the two models as we vary p , the probability we move in the same direction as the previous day. We show $\mathbb{V}[Y_T]/\mathbb{V}[X_T]$ in

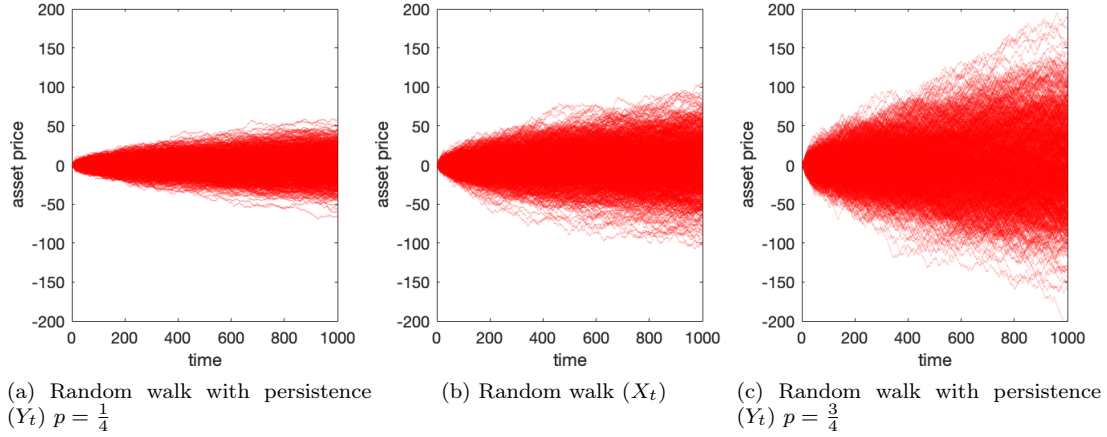


Figure 1: Simple models for asset prices

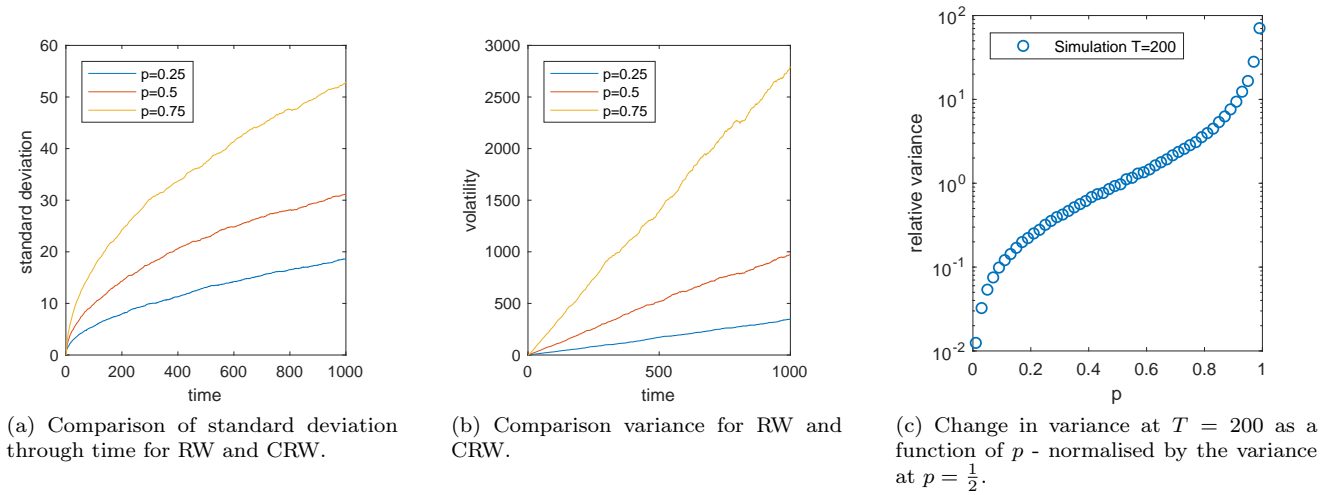


Figure 2: Comparison of measures of uncertainty for two models.

Figure 2c where $T = 200$ is the final day. Interestingly, we see that over a broad range of p , e.g. $p \in [0.2, 0.8]$ then the relative increase in variance is approximately linear in the log-scale (suggesting it is exponential in p) and for p close to 1 the relative increase in volatility rises super-exponentially. We note, that the variance reduces for $p < 0.5$ as in this case the model of CRW if the last move was down (for example) the next move will be up with high probability and so as $p \rightarrow 0$ then the asset price tends to something that alternates between 0 and +1 or 0 and -1. Finally, assuming that in both cases the variance is approximately linear in time, we are able to take the ratio of the volatilities between the two to give some measure of the relative change in variance per unit of time as well.

3 Application to daily data

We here introduce a semiparametric model for a price process, relaxing the assumption that the increments must be in $\{-1, +1\}$ to a more general class of return distributions. We consider discretely observed price processes, with consideration of continuous-time processes to follow.

We assume, as before, that the sign of the increment is governed by a correlated random walk model, with increments taking values in $\{-1, 1\}$, which we denote as (S_n) . Conditional on S_{n-1} , then $S_n = S_{n-1}$ with probability p and $S_n = -S_{n-1}$ with probability $1 - p$. Coupled with this, we also introduce random variables representing the magnitude of the change in price at each iteration, which we denote as (δ_n) . The overall price process may then be expressed as

$$Z_n = \sum_{i=0}^n S_i \delta_i \quad (1)$$

where $\delta_i \geq 0$ are random variables used to model an increment of an arbitrary price process. We assume that conditional on a realisation of $(S_i)_{i=0}^n$ the increments are conditionally independent, with $\delta_i \stackrel{i.i.d.}{\sim} \nu$ for some distribution ν .

Proposition 1. *For S_0 symmetrically distributed on $\{-1, 1\}$ and $\mathbb{E}_\nu[\delta^2] < \infty$, the limiting variance of the proposed price process satisfies*

$$\lim_{n \rightarrow \infty} \frac{1}{n} \mathbb{V}[Y_n] = \mathbb{E}_\nu[\delta^2] + \mathbb{E}_\nu[\delta]^2 \left(\frac{2p - 1}{1 - p} \right) \quad (2)$$

where \mathbb{E}_ν denotes the expectation of a random variable distributed according to ν .

Proof is in Appendix A.1. Previous expressions for limiting variance of a correlated random walk model can be found in [Renshaw and Henderson, 1981, Mauldin et al., 1996, Guo et al., 2017], though without the additional complexity arising from a random magnitude distribution ν .

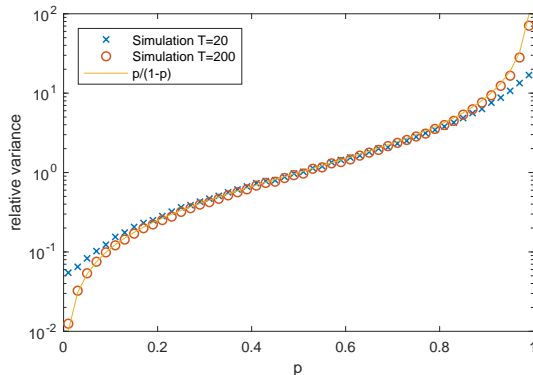


Figure 3: Change in variance at $T = 200$ as a function of p . Shown also is the change in variance as a function of p for $T = 20$ where we see that the change the solution $p/1 - p$ breaks down in the tails though captures the central part well.

Considering Equation (2), we see that for a magnitude distribution ν concentrated on a single (strictly positive) point x , then the $\mathbb{E}_\nu[\delta^2] = \mathbb{E}_\nu[\delta]^2$ and the limiting variance is

$$\lim_{n \rightarrow \infty} \frac{1}{n} \mathbb{V}[Y_n] \propto \frac{p}{1-p} \quad (3)$$

thereby capturing the previous analysis as a special case. Indeed, we see that in this case for $p > \frac{1}{2}$ then the the variance is increased and for $p < \frac{1}{2}$ the reverse is true, indeed the variance is a monotonically increasing function of p . We compare the change in variance as a function of p with the previous simulation estimates, overlaying the analytical solution in Figure 3. We see that $p/1 - p$ fits the experiment exceptionally well for $T = 200$. Additionally we see that for $T = 20$ the fit is less good in the extremal values of p though still permissible. Such a result suggests that the result is indeed asymptotic (i.e. the change in variance is not necessarily $p/1 - p$ over a small period) though in any case we expect the long run behaviour to better capture the current dynamics of an asset price. Finally, we also see according to Proposition 1 that a random walk model can be recovered through setting $p = \frac{1}{2}$, in which case $\lim_{n \rightarrow \infty} \frac{1}{n} \mathbb{V}[Y_n] = \mathbb{E}_\nu[\delta^2]$.

3.1 Model estimation

The model proposed in (1) depends on a parameter p , modelling the distribution of the sign process, and the magnitude of the returns $(\delta_n)_{n \geq 0}$. We see that the sequence $(S_n)_{n \geq 0}$ is an observable Markov chain parameterised by p - where p can be estimated through the proportions of consecutive S_n that share the same sign. The following will make no further assumptions on the distribution of ν , the magnitude distribution, beyond the previously mentioned condition that $\mathbb{E}_\nu[\delta^2] < \infty$.

3.2 US stock data

We exploit Proposition 1 to find the relative increase in variance of asset prices arising from persistence in trading directions. We focus primarily on the US stock market, in particular focussing on some of the largest stocks available for trading. We restrict attention to those stocks with traded volume greater than or equal to 100,000 and extract daily closing data for the 100 largest stocks (sorted by market capitalisation). A complete list of these stocks is available in the Appendix A.4 and the market cap. for the largest 20 is shown in Figure 4.

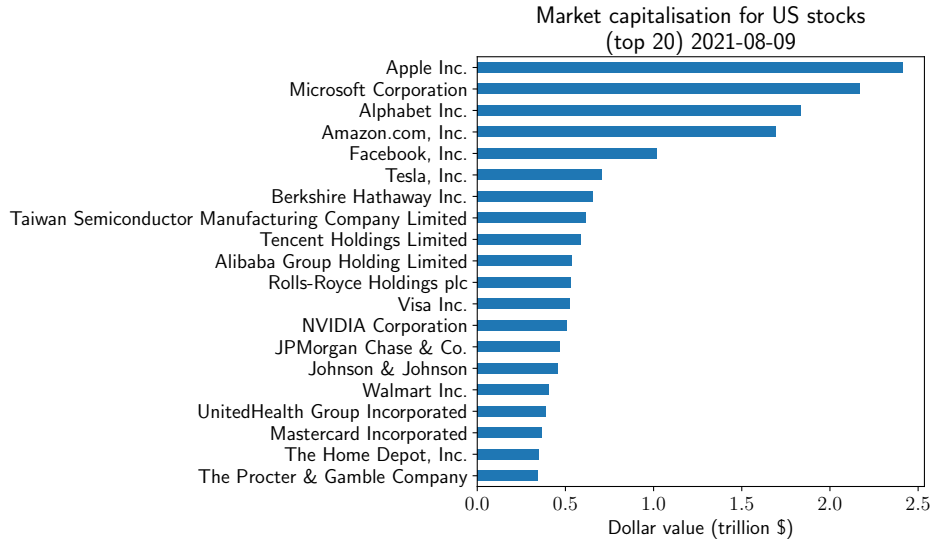


Figure 4: Market capitalisation for largest 20 stocks.

The time period considered was three years of daily data from 9th August 2018 to 9th August 2021, with data extracted from Yahoo Finance, using `yfinance` Python package. A modest amount of filtering was performed to ensure only suitable stocks were included in the analysis. In particular, two stocks were excluded based on large observed periods of no change in the price. Finally, Alphabet Inc. was duplicated with GOOGL and GOOG ticker symbols (stocks with and without voting rights) so only the largest of the two was included (GOOGL). This resulted in a total of 97 of the 100 stocks being included, a complete list of these can be found in the Appendix.

Crucial to the subsequent analysis is some guarantee that the assumptions made in Proposition 1 are reasonable. As such, we perform two model validations, checking firstly that the distribution of returns is approximately symmetric and secondly that the magnitude of the increments is uncorrelated with the sign of the increments. Details around these two procedures are provided in the Appendix A.3, though in summary, at a significance level of 5%, approxi-

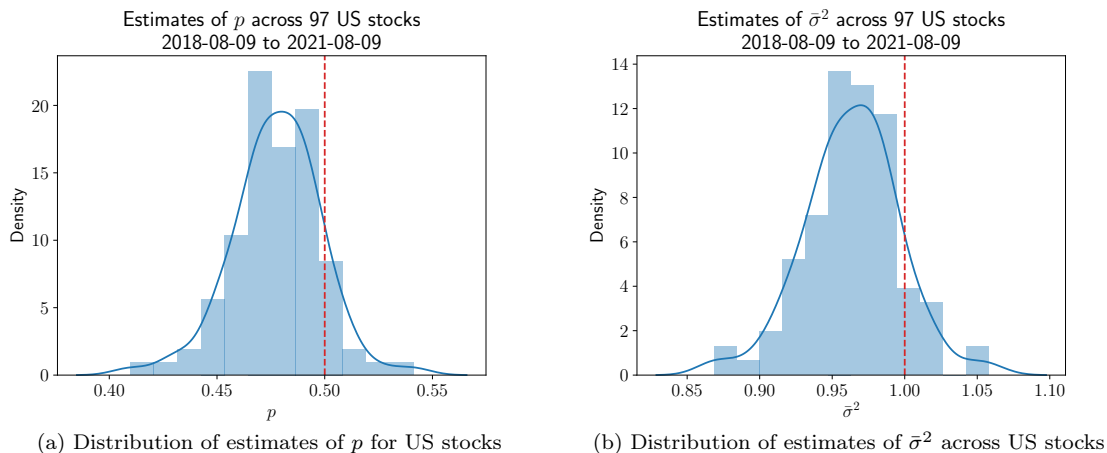


Figure 5: Inflation of variance of US stocks relative to random walk

mately 5.15% of the stocks included in the analysis did not show sufficient evidence of either asymmetric increments or increment magnitude correlated with sign.

Having performed this model validation, it is then possible to estimate the increase in variance arising from persistence in trading direction through estimating quantities appearing in Equation (2). In particular we are interested in the change in variance caused by persistent market trading. We denote this $\bar{\sigma}^2$ and express it as

$$\bar{\sigma}^2 := 1 + \frac{\mathbb{E}_\nu[\delta]^2}{\mathbb{E}_\nu[\delta^2]} \left(\frac{2p - 1}{1 - p} \right)$$

Estimates of $\mathbb{E}_\nu[\delta^2]$ and $\mathbb{E}_\nu[\delta]$ are obtained through sample averages of the distribution of magnitudes of the price process. Return increments were taken as additive on the log-scale, so that $\delta_i = |\log(Z_i) - \log(Z_{i-1})|$. Based on estimates of $\mathbb{E}_\nu[\delta^2]$, $\mathbb{E}_\nu[\delta]$ and p from historical data we are able to compare the inflated variance due to persistence with the natural variance arising from a random walk model.

In Figure 5a we show the estimated values of p across the 97 stocks under consideration. Adjacent to this we show the distribution of variances, normalised by the variance of a random walk model. Strikingly we see that typical values of p are less than $\frac{1}{2}$ and the variance of the assets are actually *deflated*. Such a result suggests that in some of the world's largest stocks, the freneticism apparent in the market actually serves to make the resulting processes *more* predictable - their variance is lower. Specifically we see that the median value of $\bar{\sigma}^2$ is 0.965, with lower and upper quartile given by 0.946 and 0.982 respectively. In summary, we see that there is approximately a 1.7-5.4% *reduction* in variance due to persistence in trading directions.

4 Application to high-frequency data

In addition to the discrete-time analysis in the previous section we also develop methodology capable of learning p in a flexible model of high-frequency data. Such a model may also be applicable to highly illiquid assets, exhibiting only occasional changes in price.

As a result, rather than considering trades occurring at regular intervals we assume the times at which a price changes is itself a stochastic process. The resulting model falls under the class of Markov renewal processes [Pyke, 1961]. They are closely related to the continuous time random walks of [Kotulski, 1995, Tunaley, 1974, Scalas, 2006a]. In the physics literature continuous time random walks have found applications in econophysics and finance, see [Scalas, 2006a,b] for some summarising results illustrating the deep connection between continuous time random walks and fractional calculus. We show in Appendix A.2 that much of the previous analysis in discrete time generalises to this setting under the critical assumption that the arrival times between events are independent of the sign and magnitude process.

4.1 A high-frequency model

As remarked in [Scalas, 2006a], the distribution increments of event times is typically coupled to the distribution of jumps. The following proposes a general model motivated by the previous analysis to allow for a more flexible distribution over inter-event times and jump values. Importantly, despite the additional sophistication, the model remains interpretable and retains a probability parameter p of moving in the same direction as the previous iteration.

To better capture the dynamics at higher frequencies, where the time between events is itself a random variable, we model jointly the price process and the time-to-event process. Let Z_t denote the state of the process at time t . Then with τ_n denoting the time between events $n - 1$ and n , and (S_n, δ_n) denoting the sign and magnitude process defined previously, then the process at iteration n evolves as follows

$$S_n | \{S_{n-1} = s_{n-1}\} \sim P(\cdot | s_{n-1}) \quad (4)$$

$$(\delta_n, \tau_n) | \{S_n = s_n, S_{n-1} = s_{n-1}\} \sim f(\cdot | s_n, s_{n-1}) \quad (5)$$

where $P(\cdot | s)$ denotes the Markov transition kernel corresponding to the previous defined Markov sign process. The additional distribution f specifies the joint distributions over the increments of the price process and the increments of time-to-event process. The final price process is then given as

$$Z_t = \sum_{i=1}^{N(t)} S_i \delta_i \quad \text{where} \quad N(t) = \sup\{n : \sum_{i=1}^n \tau_i \leq t\}$$

with the latter denoting the counting process.

Analogously to the simplified model, using p we are able to control the direction of the price

process (either positive or negative) with sizes of the increment specified by the more flexible distribution f .

Where possible, we opt to use the empirical distribution of historical increments, in particular, to define the choice of f . Based on this model, we are able to construct a flexible model capable of simulating from (4) and (5) through selecting f to be the empirical distribution of (δ_n, τ_n) conditioned such that

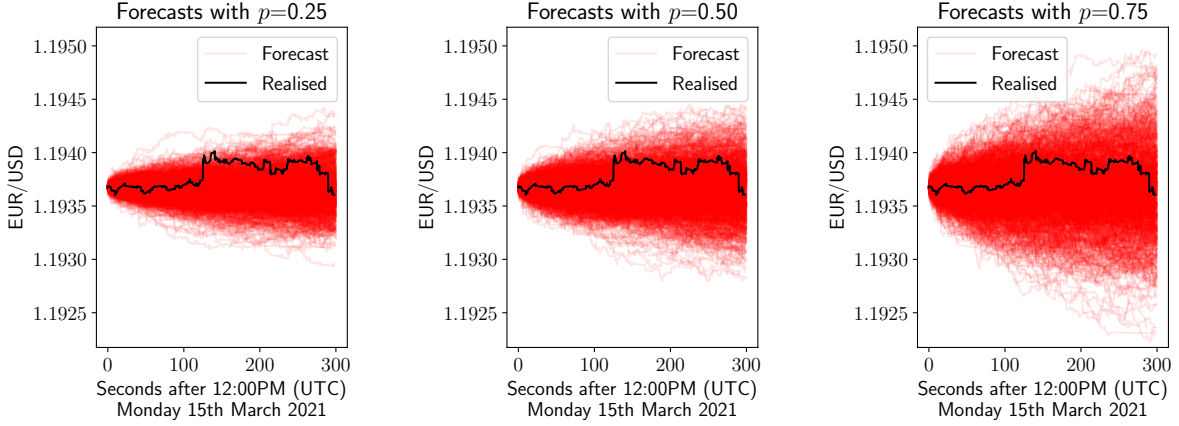
$$(\delta_n, \tau_n) | (s_n, s_{n-1}) \sim \begin{cases} \hat{F}(\{\delta_n, \tau_n : \delta_n > 0, \delta_{n-1} > 0\}) & \text{if } s_n = 1, s_{n-1} = 1 \\ \hat{F}(\{\delta_n, \tau_n : \delta_n > 0, \delta_{n-1} \leq 0\}) & \text{if } s_n = 1, s_{n-1} = -1 \\ \hat{F}(\{\delta_n, \tau_n : \delta_n \leq 0, \delta_{n-1} > 0\}) & \text{if } s_n = -1, s_{n-1} = 1 \\ \hat{F}(\{\delta_n, \tau_n : \delta_n \leq 0, \delta_{n-1} \leq 0\}) & \text{if } s_n = -1, s_{n-1} = -1 \end{cases} \quad (6)$$

where we use $\hat{F}(\{x_i\})$ denote the empirical distribution function of datapoints $\{x_i\}$.

4.1.1 Forecasting high-frequency EUR/USD

We fit the model to two weeks of high-frequency EUR/USD commencing 8th March 2021, where week 1 was used as data to estimate the empirical distribution in (6) and where week 2 was used to assess the quality of wthe forecasts. The high-frequency data was provided by the Dukascopy exchange and partially discretised, so that the minimum time between events was 0.05s.

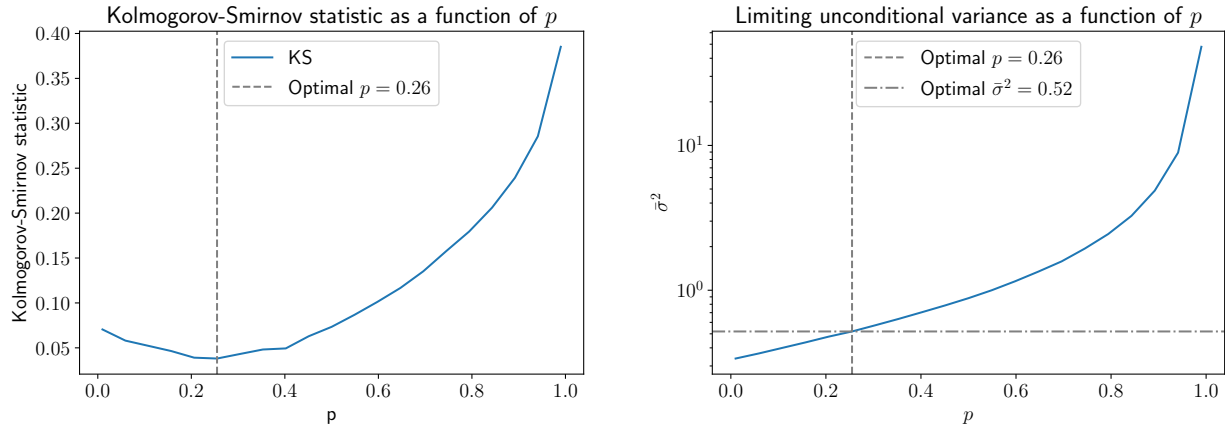
Initially, we plot forecasts from the model in 6 where we plot realisations from the model for 5 minutes after midday on 15th March 2021. We do this for three values of p and using the previous week to estimate the empirical distribution in (6). We can see that the variance is increasing as p increases, consistent with the continuous time random walk model.



(a) Forecasts & historical data $p = \frac{1}{4}$ (b) Forecasts & historical data $p = \frac{1}{2}$ (c) Forecasts & historical data $p = \frac{3}{4}$

Figure 6: Forecast plots

Subsequently, we assess the performance of the model at forecasting through a simulation based approach in the spirit of [Andersen et al., 2003]. For a given value of p , such an approach iteratively performs Monte Carlo simulations to obtain the distribution of price process at a given time point. Let $\{\hat{Z}_t^{(i)}\}$ represent the predicted distribution of the process Z_t at time t . As in [Andersen et al., 2003], we are then able to construct a statistic through taking the probability integral transform of Z_t through the empirical distribution function $\hat{F}(\{\hat{Z}_t^{(i)}\})$, which will be approximately uniformly distributed if the predictions are accurate. For varying values of p , we assess the quality of forecast predictions using the Kolmogorov-Smirnov distance of the probability integral transforms from the uniform distribution. Forecasts were made every 5 minutes over periods of 5 minutes from Monday 0:00AM (UTC) 15th March 2021 to Saturday 0:00AM (UTC) 20th March 2021. Figure 7a shows how the Kolmogorov-Smirnov distance (our measure of prediction accuracy) varies as p varies, using 100,000 Monte Carlo simulations. We see that there is a clear minimum at $p = 0.26$. We cross-reference this with the variance predicted by the model through simulations at varying levels of p , shown in Figure 7b, where we see that the variance is less than the variance in the absence of these correlations ($p = 0.5$), to the extent that it is deflated to approximately 52% of the variance without correlations. Indeed we see that over this week the prevailing trading style is most likely therefore mean-reverting.



(a) Measure of forecast quality (lower the better) as a function of p

(b) Variance for EUR/USD as a function of p

Figure 7: Fitting the model to a week of EUR/USD data and predicting on the subsequent week.

5 Discussion and conclusion

We have explored using a probabilistic model for investment styles to show that the variance of a financial asset is directly dependent on the probability of moving in the same direction on successive days. The theoretical analysis shows that variance may actually be reduced through reversal strategies - capturing the case that the asset is more likely to move in opposing directions on subsequent days. We have applied a simple model to US stock data, showing that such a regime is indeed prevalent in 97 of the largest stocks and thereby proven that relative to a random walk the variance of these stocks is actually *reduced* as a result of this frenetic behaviour. Indeed such a result suggests that these stocks are actually *more* predictable than a random walk due to this artefact. A similar result is also shown for higher-frequency data in the case of the EUR/USD to a more exaggerated extent. Similar ideas have been explored from a different perspective with the identification of a Hurst exponent of a stochastic process, quantifying the asymptotic behaviour of the range of a stochastic process [Qian and Rasheed, 2004], though in general describe the behaviour only qualitatively.

The models considered above allow for many more flexible generalisations. In particular, [LeBaron, 1992] remarks that period of high volatility are typically occur during periods of low autocorrelation (and vice verser). It would be interesting to allow for variable volatility in the above model, exploring dynamically changing correlation parameters p . Alternatively, it would also be interesting to consider the sign process for multiple assets simultaneously rather than

focussing - as is the case here - on a single asset. Similarly, it may be fruitful to consider a sign process where subsequent values depend on more than one lag of the process, thereby providing a still more flexible model. Finally, a principled incorporation of processes exhibiting long-term drift would also provide additional insight into asset price behaviour.

More generally, that autocorrelation contributes to larger variance is well known within the computational statistics literature. In particular, the autocorrelation in a class of algorithms referred to as Markov chain Monte Carlo algorithms typically serves to increase the variance arising from the Monte Carlo noise [Robert and Casella, 2013] in a directly analagous fashion to the increase in variance as defined above.

References

- Torben G Andersen, Tim Bollerslev, Francis X Diebold, and Paul Labys. Modeling and forecasting realized volatility. *Econometrica*, 71(2):579–625, 2003.
- Louis KC Chan, Narasimhan Jegadeesh, and Josef Lakonishok. Momentum strategies. *The Journal of Finance*, 51(5):1681–1713, 1996.
- Eugene F Fama. Random walks in stock market prices. *Financial analysts journal*, 51(1):75–80, 1995.
- Xin Guo, Adrien De Larrard, and Zhao Ruan. Optimal placement in a limit order book: an analytical approach. *Mathematics and Financial Economics*, 11(2):189–213, 2017.
- Narasimhan Jegadeesh and Sheridan Titman. Profitability of momentum strategies: An evaluation of alternative explanations. *The Journal of finance*, 56(2):699–720, 2001.
- Marcin Kotulski. Asymptotic distributions of continuous-time random walks: a probabilistic approach. *Journal of statistical physics*, 81(3-4):777–792, 1995.
- Blake LeBaron. Some relations between volatility and serial correlations in stock market returns. *Journal of Business*, pages 199–219, 1992.
- Burton G Malkiel. The efficient market hypothesis and its critics. *Journal of economic perspectives*, 17(1):59–82, 2003.
- Burton G Malkiel and Eugene F Fama. Efficient capital markets: A review of theory and empirical work. *The journal of Finance*, 25(2):383–417, 1970.
- R Daniel Mauldin, Michael Monticino, and Heinrich von Weizsäcker. Directionally reinforced random walks. *Advances in Mathematics*, 117(2):239–252, 1996.
- Ronald Pyke. Markov renewal processes: definitions and preliminary properties. *The Annals of Mathematical Statistics*, pages 1231–1242, 1961.
- Bo Qian and Khaled Rasheed. Hurst exponent and financial market predictability. *IASTED conference on Financial Engineering and Applications, Cambridge, MA*, 1(1):1–1, 2004.
- Eric Renshaw and Robin Henderson. The correlated random walk. *Journal of Applied Probability*, 18(2):403–414, 1981.
- Christian Robert and George Casella. *Monte Carlo statistical methods*. Springer Science & Business Media, 2013.
- Enrico Scalas. The application of continuous-time random walks in finance and economics. *Physica A: Statistical Mechanics and its Applications*, 362(2):225–239, 2006a.

Enrico Scalas. Five years of continuous-time random walks in econophysics. In *The complex networks of economic interactions*, pages 3–16. Springer, 2006b.

Martin Sewell. History of the efficient market hypothesis. *Rn*, 11(04):04, 2011.

JKE Tunaley. Asymptotic solutions of the continuous-time random walk model of diffusion. *Journal of Statistical Physics*, 11(5):397–408, 1974.

A Appendix

A.1 Proof of Proposition 1

We analyse first of all, the increment process defined as

$$Z_n = \sum_{i=1}^n S_i \delta_i$$

$S_i \in \{-1, 1\}$. By symmetry we have that $\mathbb{E}[Z_n] = 0$, so that the variance is given as

$$\mathbb{V}[Y_n] = \mathbb{E} \left[\left(\sum_{i=1}^n S_i \delta_i \right)^2 \right] \quad (7)$$

$$= \mathbb{E} \left[\sum_{i=1}^n \left((S_i \delta_i)^2 + 2 \sum_{j=1}^{i-1} \delta_i S_i \delta_j S_j \right) \right] \quad (8)$$

$$. = \mathbb{E}_\nu[\delta^2] \sum_{i=1}^n \mathbb{E}[S_i^2] + 2\mathbb{E}_\nu[\delta]^2 \sum_{i=1}^n \sum_{j=1}^{i-1} \mathbb{E}[S_i S_j] \quad (9)$$

where the final line follows from independence of the magnitudes δ_i .

We state the n -step transition matrix of S_n as

$$P^n = \frac{1}{2} \begin{pmatrix} 1 + \delta^n & 1 - \delta^n \\ 1 - \delta^n & 1 + \delta^n \end{pmatrix}$$

where $[P^n]_{ab} = \mathbb{P}[S_n = 2a - 1 | S_1 = 2b - 1]$ and $\delta := 2p - 1$ for $(a, b) \in \{0, 1\}^2$. We see this by induction in that

$$P^1 = \begin{pmatrix} p & 1-p \\ 1-p & p \end{pmatrix} = \frac{1}{2} \begin{pmatrix} 1 + \delta & 1 - \delta \\ 1 - \delta & 1 + \delta \end{pmatrix}$$

and

$$\begin{aligned} P^n P &= \frac{1}{2} \begin{pmatrix} 1 + \delta^n & 1 - \delta^n \\ 1 - \delta^n & 1 + \delta^n \end{pmatrix} \frac{1}{2} \begin{pmatrix} 1 + \delta & 1 - \delta \\ 1 - \delta & 1 + \delta \end{pmatrix} \\ &= \frac{1}{4} \begin{pmatrix} (1 + \delta)(1 + \delta^n) + (1 - \delta)(1 - \delta^n) & (1 - \delta)(1 + \delta^n) + (1 + \delta)(1 - \delta^n) \\ (1 + \delta)(1 - \delta^n) + (1 - \delta)(1 + \delta^n) & (1 - \delta)(1 - \delta^n) + (1 + \delta)(1 + \delta^n) \end{pmatrix} \\ &= \frac{1}{4} \begin{pmatrix} 2 + 2\delta^{n+1} & 2 - 2\delta^{n+1} \\ 2 - 2\delta^{n+1} & 2 + 2\delta^{n+1} \end{pmatrix} = P^{n+1} \end{aligned}$$

We have that $\mathbb{E}[S_i^2] = 1$ and by symmetry we see that

$$\begin{aligned}\mathbb{E}[S_i S_j] &= \mathbb{E}[S_i \mathbb{E}[S_j | S_i]] \\ &= 2 \left(\frac{1 + \delta^{j-i}}{2} - \frac{1 - \delta^{j-i}}{2} \right) \frac{1}{2} = (2p - 1)^{j-i}\end{aligned}$$

so that from Equation (7) we have

$$\begin{aligned}\mathbb{V}[Y_n] &= n\mathbb{E}_\nu[\delta^2] + 2\mathbb{E}_\nu[\delta]^2 \sum_{i=1}^n \sum_{j=1}^{i-1} (2p - 1)^{j-i} \\ &= n\mathbb{E}_\nu[\delta^2] + \mathbb{E}_\nu[\delta]^2 \sum_{i=1}^n \left(\frac{(2p - 1) - (2p - 1)^i}{1 - p} \right)\end{aligned}\tag{10}$$

Which, after rescaling, we see that

$$\begin{aligned}\lim_{n \rightarrow \infty} \frac{1}{n} \mathbb{V}[Y_n] &= \mathbb{E}_\nu[\delta^2] + \mathbb{E}_\nu[\delta]^2 \frac{2p - 1}{1 - p} - \lim_{n \rightarrow \infty} \frac{1}{n} \sum_{i=1}^n \frac{(2p - 1)^i}{1 - p} \\ &= \mathbb{E}_\nu[\delta^2] + \mathbb{E}_\nu[\delta]^2 \left(\frac{2p - 1}{1 - p} \right)\end{aligned}$$

where the final term tends to 0 as $x^n/n \rightarrow 0$ for $|x| \leq 1$.

A.2 Analysis of a high-frequency model

We define the times at which the direction changes as a renewal process, i.e. we assume the time between successive events is itself a random variable, which we denote by τ_1, τ_2, \dots . We define a counting process as $N(t) = \sup\{n : \sum_{i=1}^n \tau_i \leq t\}$. Considering the definition of the Markov sign process (S_n) and magnitude increments (δ_n) as before, the resulting process is then expressed as

$$Z_t = \sum_{i=1}^{N(t)} S_i \delta_i.$$

The analysis of a daily model, can be seen as a special case where for all i , τ_i is deterministically set equal to 1.

We are interested in how the parameter p affects the long-run variance of the resulting stochastic process. As a result, we define the limiting variance as

$$\bar{\sigma}^2 := \lim_{t \rightarrow \infty} \mathbb{V} \left[\frac{1}{\sqrt{t}} Z_t \right]$$

Following a similar analysis as for Proposition 1, we are able to provide an analogous expression

for the limiting variance as follows.

Theorem 1. *Under the same assumptions as Proposition 1, then assuming $(\tau_i)_{i \geq 1}$ are independent of $(S_i)_{i \geq 1}, (\delta_i)_{i \geq 1}$ and $\mu_\tau := \lim_{t \rightarrow \infty} \mathbb{E}_N \left[\frac{N(t)}{t} \right] < \infty$, we have that the limiting variance is*

$$\bar{\sigma}^2 = \mu_\tau \left(\mathbb{E}_\nu[\delta^2] + \mathbb{E}_\nu[\delta]^2 \left(\frac{2p-1}{1-p} \right) \right) \quad (11)$$

We allow for quite a general structure on the arrival time process, noting they do not necessarily exhibit finite variance and are not necessarily i.i.d. (they could themselves be a Markov process for example). From Theorem 1, we see (as before) that Equation (11) can be simplified in the special case of a deterministic magnitude distribution, suggesting

$$\bar{\sigma}^2 \propto \frac{p}{1-p}$$

providing a parallel with the discrete-time process.

Proof. Considering now the Markov renewal process Z_t , and defining $\mu_\tau := \lim_{t \rightarrow \infty} \mathbb{E}_N \left[\frac{N(t)}{t} \right]$, we are able to condition on $N(t) = n$ and take expectations so that

$$\begin{aligned} \mathbb{V} \left[\frac{1}{\sqrt{t}} Z_t \right] &= \mathbb{E} \left[\left(\frac{1}{\sqrt{t}} \sum_{i=1}^{N(t)} W_i \right)^2 \right] \\ &= \mathbb{E}_N \left[\mathbb{E} \left[\frac{1}{t} \left(\sum_{i=1}^n W_i \right)^2 \mid N(t) = n \right] \right] \\ &= \mathbb{E}_N \left[\frac{N(t)}{t} \mathbb{E}_\nu[\delta^2] + \frac{N(t)}{t} \mathbb{E}_\nu[\delta]^2 \frac{2p-1}{1-p} - \frac{1}{t} \mathbb{E}_\nu[\delta]^2 \sum_{i=1}^{N(t)} \frac{(2p-1)^i}{1-p} \right] \\ &= \mathbb{E}_N \left[\frac{N(t)}{t} \right] \left(\mathbb{E}_\nu[\delta^2] + \mathbb{E}_\nu[\delta]^2 \left(\frac{2p-1}{1-p} \right) \right) - \mathbb{E}_\nu[\delta]^2 \mathbb{E}_N \left[\frac{1}{(1-p)t} \sum_{i=1}^{N(t)} (2p-1)^i \right] \\ &= \mathbb{E}_N \left[\frac{N(t)}{t} \right] \left(\mathbb{E}_\nu[\delta^2] + \mathbb{E}_\nu[\delta]^2 \left(\frac{2p-1}{1-p} \right) \right) + \mathbb{E}_\nu[\delta]^2 \mathbb{E}_N \left[\frac{1}{t} \frac{(1-2p)}{(1-p)2p} \left(1 - (2p-1)^{N(t)} \right) \right] \end{aligned} \quad (12)$$

We have by Jensen's inequality and the triangle inequality

$$\begin{aligned} \left| \mathbb{E}_N \left[\frac{1}{t} \frac{(1-2p)}{(1-p)2p} \left(1 - (2p-1)^{N(t)} \right) \right] \right| &\leq \frac{1}{t} \left| \frac{(1-2p)}{(1-p)2p} \right| \mathbb{E}_N \left[\left| \left(1 - (2p-1)^{N(t)} \right) \right| \right] \\ &\leq \frac{1}{t} \left| \frac{(1-2p)}{(1-p)2p} \right| \mathbb{E}_N \left[1 + \left| (2p-1)^{N(t)} \right| \right] \\ &\leq \frac{1}{t} \left| \frac{(1-2p)}{(1-p)p} \right| \end{aligned}$$

as $|(2p-1)^{N(t)}| \leq 1$ we have that. As such, continuing from equation (12) we have the limiting variance given by

$$\lim_{t \rightarrow \infty} \mathbb{V} \left[\frac{1}{\sqrt{t}} Z_t \right] = \mu_\tau \left(\mathbb{E}_\nu[\delta^2] + \mathbb{E}_\nu[\delta]^2 \left(\frac{2p-1}{1-p} \right) \right).$$

□

A.3 US daily stock model validation

We here describe the model validation used to justify the model proposed in Equation (1) for US daily stock data. In particular we check

1. The empirical distribution of δ_i is symmetric
2. The observed δ_i are uncorrelated with S_i

Strictly speaking, we should investigate independence between (δ_i) and (S_i) though test for correlation for convenience. To test whether the empirical distribution of δ_i is symmetric, we employ the two-sample Kolmogorov-Smirnov test on increments of the log-price process that are non-negative against those that are non-positive. Of the 97 tests performed 5.15% of those were significant at 5%, which is perhaps a little high, though within acceptable tolerance. To test the correlation between between (δ_i) and (S_i) we estimate the p -value corresponding to Pearson's correlation. In this case, of the 97 tests performed 2.06% were significant at 5% thereby not providing evidence to reject the null that the two samples are uncorrelated.

A.4 US daily stock data

Summary data of the 100 large market capitalisation US stocks is provided in Table 1 and 2.

Symbol	Name	Price (intraday)	Volume	Market cap (\$)
AAPL	Apple Inc.	146.09	48.802M	2.415T
MSFT	Microsoft Corporation	288.33	13.927M	2.167T
GOOGL	Alphabet Inc.	2,738.26	857,805	1.834T
AMZN	Amazon.com, Inc.	3,341.87	2.035M	1.692T
FB	Facebook, Inc.	361.61	7.543M	1.02T
TSLA	Tesla, Inc.	713.76	14.543M	706.633B
BRK-B	Berkshire Hathaway Inc.	287.23	3.67M	656.99B
TSM	Taiwan Semiconductor Manufacturing Company Limited	118.22	4.007M	613.089B
TCEHY	Tencent Holdings Limited	60.55	7.093M	587.49B
BABA	Alibaba Group Holding Limited	195.25	14.287M	537.918B
JPM	JPMorgan Chase & Co.	157.33	8.961M	470.127B
V	Visa Inc.	240.00	5.161M	526.654B
NVDA	NVIDIA Corporation	202.95	13.289M	505.751B
JNJ	Johnson & Johnson	173.71	3.801M	457.288B
WMT	Walmart Inc.	145.58	5.259M	407.937B
BAC	Bank of America Corporation	40.67	48.111M	342.234B
UNH	UnitedHealth Group Incorporated	410.87	1.466M	387.416B
MA	Mastercard Incorporated	370.68	2.362M	365.778B
HD	The Home Depot, Inc.	328.76	1.876M	349.557B
PG	The Procter & Gamble Company	142.18	4.352M	345.455B
RHHBY	Roche Holding AG	49.07	1.145M	342.978B
NSRGY	Nestlé S.A.	123.50	131,247	342.528B
PYPL	PayPal Holdings, Inc.	278.15	3.706M	326.835B
ASML	ASML Holding N.V.	788.68	472,372	325.107B
DIS	The Walt Disney Company	176.66	4.926M	320.979B
ADBE	Adobe Inc.	629.22	996,552	299.76B
NKE	NIKE, Inc.	171.77	3.396M	271.706B
CMCSA	Comcast Corporation	58.28	12.086M	267.49B
PFE	Pfizer Inc.	45.98	30.369M	257.382B
LLY	Eli Lilly and Company	267.16	2.791M	255.56B
TM	Toyota Motor Corporation	180.57	155,646	252.233B
ORCL	Oracle Corporation	89.90	5.678M	251.001B
KO	The Coca-Cola Company	56.65	8.185M	244.537B
CRM	salesforce.com, inc.	249.32	3.298M	242.222B
XOM	Exxon Mobil Corporation	57.20	15.209M	242.16B
CSCO	Cisco Systems, Inc.	55.47	6.963M	233.762B
NVO	Novo Nordisk A/S	100.65	1.031M	231.352B
NFLX	Netflix, Inc.	519.97	1.302M	230.137B
VZ	Verizon Communications Inc.	55.12	12.064M	228.203B
DHR	Danaher Corporation	307.97	1.368M	219.86B
INTC	Intel Corporation	54.04	14.204M	219.24B
ABT	Abbott Laboratories	123.16	4.265M	218.341B
WFC-PO	Wells Fargo & Company	25.27	120,697	213.443B
PEP	PepsiCo, Inc.	154.35	2.188M	213.329B
TMO	Thermo Fisher Scientific Inc.	541.16	831,562	212.691B
NVS	Novartis AG	91.81	1.226M	207.074B
ACN	Accenture plc	319.52	1.205M	202.619B
ABBV	AbbVie Inc.	114.06	5.201M	201.565B

Table 1: 100 largest US stocks by market capitalisation 2021-08-09

Symbol	Name	Price (intraday)	Volume	Market cap (\$)
WFC	Wells Fargo & Company	48.65	26.408M	199.777B
AVGO	Broadcom Inc.	484.68	569,893	198.845B
VWDRY	Vestas Wind Systems A/S	13.18	241,291	198.801B
T	AT&T Inc.	27.85	21.162M	198.849B
MRNA	Moderna, Inc.	484.47	41.879M	195.554B
COST	Costco Wholesale Corporation	440.47	1.244M	194.718B
BHP	BHP Billiton Limited	76.54	979,561	194.584B
SHOP	Shopify Inc.	1,549.99	1.083M	194.256B
CVX	Chevron Corporation	100.25	8.423M	193.874B
MRK	Merck & Co., Inc.	75.32	7.175M	190.715B
SBRCY	Sberbank of Russia	17.70	138,498	184.988B
CICHY	China Construction Bank Corporation	14.17	194,040	180.599B
C	Citigroup Inc.	71.52	14.185M	144.956B
TMUS	T-Mobile US, Inc.	142.99	3.012M	178.447B
MPNGY	Meituan	57.56	111,865	176.389B
MS	Morgan Stanley	100.74	8.091M	183.806B
TXN	Texas Instruments Incorporated	190.45	2.315M	175.825B
AZN	AstraZeneca PLC	56.36	9.63M	175.727B
MCD	McDonald's Corporation	234.68	1.858M	175.259B
SAP	SAP SE	146.56	463,896	174.447B
VWAGY	Volkswagen AG	34.79	437,040	174.401B
MDT	Medtronic plc	126.92	2.949M	170.568B
UPS	United Parcel Service, Inc.	190.98	1.752M	166.254B
QCOM	QUALCOMM Incorporated	146.92	4.536M	165.726B
BBL	BHP Group	63.80	1.161M	161.725B
PNGAY	Ping An Insurance (Group) Company of China, Ltd.	17.68	502,175	161.598B
SE	Sea Limited	307.14	1.744M	161.075B
RDS-A	Royal Dutch Shell plc	41.04	4.047M	160.118B
RDS-B	Royal Dutch Shell plc	40.35	4.187M	159.578B
NEE	NextEra Energy, Inc.	80.56	4.83M	158.039B
HON	Honeywell International Inc.	228.23	1.306M	157.57B
LIN	Linde plc	303.26	900,463	156.607B
PM	Philip Morris International Inc.	99.20	1.609M	154.607B
GS	The Goldman Sachs Group, Inc.	399.88	3.296M	134.798B
BMJ	Bristol-Myers Squibb Company	67.38	6.647M	149.726B
UL	Unilever PLC	57.26	1.25M	149.476B
INTU	Intuit Inc.	535.23	724,449	146.256B
AAGIY	AIA Group Limited	47.88	192,823	145.212B
RY	Royal Bank of Canada	102.80	562,572	147.145B
UNP	Union Pacific Corporation	219.95	1.615M	143.434B
PROSY	Prosus N.V.	17.52	1.026M	142.991B
CHTR	Charter Communications, Inc.	765.50	541,813	140.716B
SBUX	Starbucks Corporation	117.94	4.439M	139.063B
RIO	Rio Tinto plc	85.57	2.071M	138.546B
SCHW	The Charles Schwab Corporation	73.42	6.079M	138.496B
HDB	HDFC Bank Limited	75.16	629,583	138.463B
BLK	BlackRock, Inc.	901.97	276,240	137.369B
BA	The Boeing Company	232.27	8.298M	136.146B
AXP	American Express Company	170.78	2.118M	135.673B

Table 2: Largest US stocks by market capitalisation 2021-08-09